## Relative Importance of Mineralogy and Organic Matter Characteristics on Macroaggregate and Colloid Dynamics in Mg-Silicate Dominated Soils

(Article begins on next page)

25 April 2024

iris - AperTO

1 **Title**

2 **RELATIVE IMPORTANCE OF MINERALOGY AND ORGANIC MATTER CHARACTERISTICS**

3 **ON MACROAGGREGATE AND COLLOID DYNAMICS IN Mg-SILICATE DOMINATED SOILS**

4

5 **Short title**

6 **AGGREGATION IN Mg-SILICATE DOMINATED SOILS**

7

8 **Authors:**

9 Gloria Falsone [a], Luisella Celi [b], Silvia Stanchi [b,c], Eleonora Bonifacio [b]

10 [a] DIPSA – Alma Mater Studiorum University of Bologna, via Fanin 40, 40127 Bologna, Italy

11 [b] DISAFA, University of Torino, Largo P. Braccini 2, 10095 Grugliasco (TO), Italy

12 [c] NATRISK, Research Centre on Natural Risks in Mountain and Hilly Environments, University of Torino,

13 Largo P. Braccini 2, 10095 Grugliasco (TO), Italy

14

15 **Corresponding author:**

16 Eleonora Bonifacio: tel +39 011 670 8516, fax +39 011 6708692, E-mail Eleonora.Bonifacio@unito.it

17

18 <div align="center">**ABSTRACT**</div>

19 Soil aggregation and organic matter conservation are important in the prevention of land degradation.

20 Aggregation processes and organic matter turnover influence each other and depend on the characteristics of

21 both minerals and organic pools. We assessed the relative importance of the organic and mineral phases at the

22 macroaggregate and colloidal scale in two soils (CHL and SRP, chlorite and serpentine-rich, respectively)

23 where Mg-silicates dominated, by incubating them with a relatively degraded and oxidized organic fraction,

24 i.e. the humic acids (HA) extracted from the organic horizons of both CHL and SRP. The HA from SRP were

25 more aromatic and richer in phenolic groups, whereas HA from CHL were N-richer, more aliphatic and richer

26 in carboxyl groups. The SRP soil formed larger amounts of macroaggregates, more stable than in CHL. At the

27 colloidal scale, SRP was more flocculated and clay had a lower electrophoretic mobility than CHL. HA

28 enhanced aggregate formation in both samples but improved aggregate stability only in CHL. In CHL slight

29 differences in electrophoretic mobility were visible, while in SRP differences were more pronounced, with a

30 PZC at lower pH and larger hydrodynamic diameter. The abundance of Mg in SRP may have favoured the

31 formation of weaker outer-sphere interactions and the release of clay-HA associations upon water dispersion,

32 while in CHL Ca formed more stable bonds with HA. In SRP ligand exchange reactions can be ruled out,

33 conversely to the dominant bonding mechanism occurring in Al-silicate dominated soils, with important

34 consequences on the release of organic matter-loaded clay particles.

35

36 **KEYWORDS:** oxidized organic matter, aggregate stability, zeta potential, soil mineralogy, serpentine

37

**INTRODUCTION**

Soils are a finite resource sustaining terrestrial life and providing a wide set of ecosystem functions that are vital for the human kind, such as food and biomass production, carbon regulation, filtering pollutants, biodiversity and natural/cultural heritage (Adhikari & Hartemink, 2016; Berendse et al., 2015; Keesstra et al., 2012). However, soil degradation is an ongoing process often leading to permanent loss, putting at risk soil quality and availability for future generations. Land degradation is the result of a large number of natural and man-induced processes (Seeger & Ries, 2008; Zhang et al., 2015) that affect the topsoil chemical and physical quality and globally decrease soil functionality (Brevik et al., 2015). Among the main effects of land degradation, the breakdown of soil structure and disruption of aggregates are widely studied (De Clercq et al., 2015) as they are good indicators of poor soil quality (Zornoza et al., 2015). Soil structure and aggregate stability are directly impacted by land use (Cerdà, 2000; de Oliveira et al., 2015) and enhanced in natural and forest ecosystems or upon afforestation (Muñoz-Rojas et al., 2015) and tree plantation (Gümüs & Şeker, 2015). By affecting soil infiltration capacity, soil aggregates play a key role in controlling erosion processes and soil losses in semiarid areas and in areas that have lost their original vegetation cover (Arjmand Sajjadi & Mahmoodabadi, 2015; Cerdà, 1996; Mataix-Solera et al., 2011).

In addition to the well-known effect that soil structure and aggregates have on soil fertility, gas exchanges, and on the hydrological cycle, they significantly influence organic matter stocks and are thus fundamental in the carbon cycle (Six & Paustian, 2014; Chaplot & Cooper, 2015; O'Rourke et al., 2015). The inclusion of organic residues increases the stability of macroaggregates, although the highest residence time is recorded for clay-associated OM (Gelaw et al., 2013). A complex relationship between OM and aggregates therefore exists in soils: aggregation is favoured by OM, but in turn aggregates largely control the dynamics of organic pools (Six et al., 2004; Kögel-Knabner et al., 2008; Stanchi et al., 2015). Typically, OM in microaggregates is more stable and less sensitive to changes in land use (Debasish-Saha et al., 2014). Macroaggregates instead include also fresh residues that may undergo further transformation if aggregate turnover is slow enough to allow the physical protection of OM (Six et al., 2004). The addition of fresh, bio-labile organic compounds has a short term effect on soil aggregation processes, while treating the soil with more degraded and oxidized organic materials may lead to a stable improvement of soil physical characteristics (Piccolo & Mbagwu, 1999; Abiven et al., 2009; Mamedov et al., 2014; Mikutta et al., 2015). The effect of these molecules on soil aggregation depends, however, on the availability of reactive mineral surfaces and dispersion/flocculation behaviour of the colloidal fraction (Amezketa, 1999; Vogel et al., 2014). Denef et al. (2002) observed that soils with dominating variable charge clay minerals have a greater potential to form stable macroaggregates when OM concentrations are low, while the greatest response in stable macroaggregate formation with additional organic inputs was found in soils with mixed mineralogy, likely because of the occurrence of different binding mechanisms. Also the characteristics of organic material affect the mechanisms involved in the reactions with mineral surfaces by determining both bonding extent and strength (Mikutta et al., 2007). The presence of this large set of controlling variables makes the study of the effect of organic matter on aggregation challenging, and field studies are mostly limited to the description of statistical correlations (Regelink et al., 2015). Laboratory

2

75   experiments of aggregate building up may be more suitable for understanding the relative role of several

76   controlling variables without having to deal with excessive complexity, and therefore widely used to evaluate

77   the effect of different pools of organic matter on aggregation (Ding et al., 2013; Andruschkewitsch et al., 2014;

78   Vogel et al., 2014). However, most studies were carried out on kaolinites, smectites and vermiculites, or on

79   soils where these Al-silicates dominated. Magnesium-rich phyllosilicates, such as serpentines (1:1) and

80   lithogenic chlorites (2:1:1), are less frequent, but are often found in alpine regions and on peri-Alpine

81   floodplains (Legros, 1992). Due to the different chemical properties of Al and Mg, the extent of direct bonding

82   of OM to phyllosilicate surfaces should sharply differ and the results obtained with Al-silicates might not be

83   directly applied to chlorite- or serpentine-dominated soils.

84   From previous studies, we found that the aggregation process induced by water-only wet and dry cycles

85   differed in serpentinic and chloritic soils; clay-sand interactions prevailed in aggregate building up when the

86   clay fraction was dominated by serpentine, while interactions between clay particles prevailed in the chloritic

87   soil (Falsone et al., 2007). In this study, we hypothesized that the input of degraded, oxidized organic

88   substances during wet and dry cycles might promote particle aggregation depending on their characteristics

89   and soil mineralogy. The aim of this work was therefore to evaluate the relative importance of soil mineralogy

90   and of the characteristics of added OM on aggregation and aggregate stability, both at the macroaggregate and

91   colloidal size-scale. We also evaluated the differences in aggregate properties caused by the addition of organic

92   matter by comparing the results with those obtained in the previous wet and dry experiment.

93

94                     **MATERIALS AND METHODS**

95

96   *The study area*

97   The study area was located in north-western Italy (45°10'N, 7°23'E; Col del Lys). Two soils were selected in

98   the area belonging to the greenstone belt of the Alps, a complex mix of ophiolites with micaceous, chloritic

99   and calcareous schists. In the study area the soil parent material differs therefore in mineral abundance. One

100  selected soil developed from chlorite-schists (CHL), and the other one was on serpentinite (SRP). They were

101  described and classified as Typic Udorthent and Typic Hapludalf, respectively (Soil Survey Staff, 2014). The

102  dominant vegetation consisted of grassland, although some larch trees were present at SRP. Soil samples were

103  collected from the second horizon (AC and A2, respectively) after discarding the first A horizon to reduce the

104  effect of native organic matter. The amount of organic carbon was less than 30 g kg$^{-1}$ and quite similar between

105  the two soil samples; the soils differed for the dominant cation on the exchange complex (Ca in CHL and Mg

106  in SRP), in pH (5.4 vs 6.1 in CHL and SRP, respectively) and CHL was sandy-loam, while SRP was loamy.

107  Additional details can be found in Falsone et al. (2007).

108

109  *Extraction and characterization of mineral and organic phases*

110  The mineralogical composition of the samples was evaluated through X-ray diffraction using a PW1810

111  diffractometer (40kV and 20 mA, Co Kα, graphite monochromator) on both the <2 mm sieved samples and

3

112  the clay fraction. The <2 mm samples were finely ground in an agate mortar and analyzed as air-dried randomly

113  oriented powders from 3 to 80 °2θ at a speed of 0.6 °2θ min$^{-1}$. The clay fraction was separated by centrifugation

114  after addition of sodium hexametaphosphate [(NaPO$_3$)$_6$] and analyzed as air-dried, ethylene glycol solvated,

115  K-saturated, and heated (550°C) oriented mounts. Scans were made from 3 to 35 °2θ at a speed of 1 °2θ min$^-$

116  $^1$. A semiquantitative evaluation of mineral abundance was performed after background subtraction and

117  calculation of peak intensities and positions using the second derivative option of the PowderX software

118  (Dong, 1999).

119  The organic matter fraction was extracted from the organic horizons of both soils by treating the samples with

120  0.5M NaOH, followed by acidification to pH 1 with HCl and purification with a 0.1N HCl/0.3N HF solution

121  (Swift, 1996). The purified fraction, i.e. the humic acid fraction, (HA) was then washed with deionized water

122  until the solution pH was 3, freeze-dried and stored for further analysis. The two obtained HA fractions were

123  labelled as HA-CHL and HA-SRP.

124  The elemental composition (C, N, H, S) of HAs was determined with an elemental analyzer (CE Instruments

125  NA2100, Rodano, Italy); the O content was calculated by difference. The amount of total acidity and carboxyl

126  groups was determined according to Schnitzer and Gupta (1965); the amount of phenolic −OH groups was

127  calculated by difference. The absorbance ratio of HA solutions at 465 and 665 nm was used to determine the

128  $E_4/E_6$ ratio (Chen et al., 1977). The absorbance was measured with an UV-Vis spectrophotometer (U-2000,

129  Hitachi, Tokio, Japan).

130  The Fourier-Transform Infrared (FT-IR) spectra of HAs were recorded using pellets prepared by pressing 0.5

131  mg of humic substances with 200 mg of anhydrous KBr. Spectra were acquired from 4000 to 400 cm$^{-1}$, at 4

132  cm$^{-1}$ resolution and 16 scans were averaged.

133

134  *Incubation conditions*

135  One hundred grams of the <2 mm air-dried samples of each soil were evenly distributed in a container and

136  sprayed with a solution of HA containing 0.5 g of C$_{HA}$. To evaluate the effect of HA composition, each soil

137  (CHL and SRP) was incubated with both HA fractions. Four aggregation tests were thus performed: CHL plus

138  HA-CHL, CHL plus HA-SRP, SRP plus HA-CHL and SRP plus HA-SRP. The samples were allowed to dry

139  for 2 weeks at room temperature. The experiment was replicated three times. At the end of the incubation

140  period, the samples were sequentially dry sieved on 5- and 2-mm sieves, the aggregates remaining on each

141  sieve (i.e. newly formed aggregates, NF) were weighed, and the result was expressed as percentage of the total

142  mass (i.e., sum of <2, 2-5 and >5 mm fractions). The aggregation state was described by the Mean Weight

143  Diameter (MWD) computed across *n* sieve size fractions using the relation:

144  $$MWD = \sum_{i=1}^{n} \bar{x}_i \, w_i \qquad\qquad (1)$$

145  where $\bar{x}_i$ is the assumed diameter of the $i^{th}$ fraction and $w_i$ is the weight fraction retained on the $i^{th}$ sieve-size.

146  The aggregate diameter classes used in the MWD calculation were 0-2, 2-5 and 5-10 mm. The upper limit of

147  the last aggregate diameter class was fixed on the basis of the observed greatest size of the NF-aggregates.

4

148

*Characterization of newly formed aggregates*

The analyses were done on the 2-5 mm NF-aggregates. The particle size distribution was determined by the pipette method (Gee & Bauder, 1986) after: (i) dispersion with $(NaPO_3)_6$; (ii) dispersion with deionized water only. The <2 µm fractions obtained were labelled as sodium-dispersible clay (NaDC) and water-dispersible clay (WDC). A first estimate of the colloidal stability was obtained by the clay dispersion ratio (CDR) calculated as the ratio between the mass (g $kg^{-1}$) of water-dispersible and sodium-dispersible clay (WDC/NaDC). On the WDC fraction, the electrophoretic mobility (EM) as a function of pH (from 2 to 6) was measured by laser Doppler velocimetry coupled with photon correlation spectroscopy using a DELSA 440 spectrometer (Beckman Coulter Electronics, Fullerton, CA) equipped with a 5-mW HeNe laser (632.8 nm). The point of zero charge was estimated by interpolating the two pH values for which the EM values were the closest to zero. The pH of the clay suspension was measured immediately before the electrochemical measurements. The Doppler shift arising from Brownian motion was used to determine the particle diffusion coefficient, which was converted to an equivalent hydrodynamic diameter using Stokes-Einstein equation as described by Hunter (1986). All measurements were run in duplicate.

The wet 2-5 mm NF-aggregate stability (WAS) was evaluated after 10 min in rotating 0.2-mm sieves. The material remaining on the sieves was then dried and weighed. The amount of stable aggregates (>0.2 mm) was corrected for the content of coarse sand determined after $H_2O_2$ oxidation. The WAS index was calculated as follows:

$$WAS = \frac{weight\ retained - weight\ of\ coarse\ sand}{total\ sample\ weight - weight\ of\ coarse\ sand} \cdot 100 \tag{2}$$

To test the wet cohesion independently from slaking, thus regardless of the ruptures due to water saturation, 10 g of NF aggregates were gently immersed into 95% solution of ethanol for 10 min (Le Bissonnais, 1996) before being wet sieved for 10 min. Then, the amount of aggregates that had resisted the sieving ($WAS_{et}$) was determined according to the equation (2).

The cumulative pore volume curve of NF-aggregates was determined using a Hg porosimeter (Porosimeter 2000 WS equipped with a Macropore unit 120, CE Instruments, Rodano, Italy). The total volume of intruded Hg (i.e. total pore volume) was expressed on a mass basis ($V_{Hg}Tot$, $mm^3\ g^{-1}$). The cumulative curve of intruded Hg volume as a function of the pore radius was used to calculate the variation of the pore volume as a function of the log-transformed radius, finding the slope between the pore radii Ri and Rj (Bruand & Prost, 1987):

$$slope_{ij} = \frac{V_i - V_j}{\log_{10} R_j - \log_{10} R_i} \tag{3}$$

where the volumes *Vi* and *Vj* correspond to the radii *Ri* and *Rj* at two successive positions *i* and *j*. The values of the slopes were plotted against the mean log radius. The relative maxima of the slope curve indicated the most represented classes of pores. Each peak thus corresponded to a radius that was termed modal radius (expressed in µm). The volume of each modal class of pores was thus included between two minimum values of the slope, which defined the limits of the class. This data treatment typically returns a bimodal distribution.

5

183 We thus labelled the modal pore radii as Rf and Rc and attributed them to the packing of finer (clay) and
184 coarser (sand and silt), according to Fiès & Bruand (1998). The corresponding volumes of pores were labelled
185 as $V_{Hg}f$ and $V_{Hg}c$. The packing density, i.e. the volume occupied by solid particles with respect to the total
186 volume, was calculated according to Falsone & Bonifacio (2009) as:

187 $$packing\ density = \frac{particle\ mass}{particle\ density} \cdot \frac{1}{\frac{particle\ mass}{particle\ density} + volume\ of\ intruded\ Hg}$$ (4)

188 where particle density was taken equal to $2.65 \times 10^{-3}$ g mm$^{-3}$, the mass was expressed in g (100 g)$^{-1}$, the volume
189 of intruded Hg in mm$^3$ g$^{-1}$, and the resulting packing density was dimensionless. We calculated the packing
190 density of clay using the NaDC fraction from textural analyses for particle mass and the modal volume
191 corresponding to clay–clay interactions. The packing density of the sand and silt phases was also calculated,
192 following the same assumptions.

193

194 *Data analysis*
195 To evaluate the relative importance of mineralogy and OM characteristics, the results of this study were
196 matched to those obtained previously (Falsone et al., 2007) after one water-only wet-dry cycle. The parameters
197 we considered were: % of 2-5 mm NF-aggregates, wet aggregate stability indexes, CDR, porosity data, and
198 PZC and hydrodynamic diameter of WDC. The changes of each parameter were expressed as % variation
199 calculated as:

200 $$\%\ variation = \frac{parameter\ value_{NF\ HA} - parameter\ value_{NF\ WD}}{parameter\ value_{NF\ WD}} \cdot 100$$

201 where *NF HA* and *NF WD* refer to the present and previous data, respectively. Differences in the % variation
202 among samples were evaluated by means of the analysis of variance (ANOVA and Duncan's test). Before
203 analysis, the homogeneity of variances was checked using the Levene test and the normality of data through
204 the Shapiro-Wilks test. The threshold used for significance in all statistical tests was set at 0.05. All data
205 treatments were carried out using SPSS 20 (SPSS Inc., Chicago, IL).

206

207

208 **RESULTS**

209

210 *Mineralogical and soil organic matter characteristics*
211 The two samples showed similar mineralogical species but sharply differ in their proportions (Figure 1). In the
212 <2 mm fraction, serpentines were the most abundant minerals in SRP (>30%), followed by chlorite, quartz,
213 Na-feldspars (albite), amphiboles, lithogenic micas (phlogopite), K-feldspars (orthoclase) and illite. In the
214 CHL sample instead the most abundant mineral was chlorite (~20%), but large amounts of feldspars (around
215 15%, both orthoclase and albite) were present, as well as lithogenic micas (margarite), talc and amphiboles
216 (~10%). Small amounts of serpentines and quartz were found as well. More differences between the two
217 samples were visible in the clay fraction: in SRP serpentine dominated (~60%), associated with minor amounts
218 of chlorite and swelling mixed-layer minerals, with traces of amphiboles, illite and illitic mixed-layers. In CHL

6

219　chlorite was the most abundant mineral (~50%), followed by talc, serpentine, illite, chlorite-illite randomly
220　interstratified minerals and traces of amphiboles.

221　The carbon content of oxidized organic matter fractions from the CHL organic horizon was significantly lower
222　($p<0.05$, n=6) than that of SRP (Table 1), while the opposite was observed for the N content. The C/N molar
223　ratio was consequently minor in CHL, indicating a higher degree of decomposition and/or a larger
224　incorporation of N containing organic compounds. The H/C and O/C molar ratios, significantly higher in CHL
225　than in SRP ($p<0.05$, n=6), suggested a larger contribution of the cellulosic component in the former. Higher
226　H/C ratios indicate indeed that the organic matter fraction from CHL is more aliphatic than SRP, while the
227　O/C ratio specifies the presence of O−containing functional groups, such as the −OH groups in the cellulose
228　polymers and carboxyl (−COOH) groups deriving from oxidation processes. This was confirmed by chemical
229　titration and FT-IR spectra (Figure 2). The HA from CHL had more carboxyl groups than SRP, but less
230　phenolic –OH groups ($p<0.05$, n=6, Table 1). The higher acidity found in SRP was coupled to a higher $E_4/E_6$
231　ratio, indicating a lower molecular size and a higher charge/mass ratio with respect to CHL. This ratio gives
232　indeed an estimate of the molecular size and presence of charged functional groups: the higher the $E_4/E_6$ ratio,
233　the smaller the size and the higher the charge (Chen et al., 1977). Although the FT-IR spectra of HAs appeared
234　similar (Figure 2), they showed some specific differences, such as the peaks at about 1631 and 1514 $cm^{-1}$
235　(aromatic C=C stretching), more pronounced in SRP, a band at 1534 $cm^{-1}$ (-CONH- stretching of II amides)
236　visible only in CHL, and a band in the region 1060-1034 $cm^{-1}$ (polysaccharide C–O stretching) more
237　pronounced in CHL. The HA from CHL appeared therefore to be richer in cellulosic and proteinaceous
238　residues, more oxidized, with a higher content of carboxyl groups, whereas HA-SRP was more aromatic and
239　richer in phenolic groups.

240

241　*Properties of the NF- macroaggregates*
242　From 100 g of the CHL fine earth we obtained on the average 18.8 and 9.8 g of 2-5 and >5 mm NF aggregates,
243　whereas the yield was 29.7 and 15.3 g for SRP, respectively (Table 2). The MWD value was consequently
244　significantly higher ($p<0.05$, n=6) in SRP samples than in CHL. No relevant differences between the two HAs
245　were found.

246　After 10 min of wet sieving, the 2-5 mm NF aggregates of CHL were more fragile than those of SRP, with
247　WAS values of 63.0 and 71.8% on average, respectively (Table 3). However, when the initial slaking was
248　avoided, the samples had similar $WAS_{et}$ values (72.8 and 74.6% on average) showing a comparable resistance
249　against water abrasion. The total volume of Hg intruded in the pores of 2-5 mm NF aggregates ($V_{Hg}Tot$) ranged
250　from 177 to 188 $mm^3$ $g^{-1}$. The analysis of the cumulative curve of the intruded Hg volume allowed to identify
251　a bimodal distribution of pores in all samples (data not shown) attributed to the coarser particles, i.e. silt and
252　sand, and to the finer colloidal phase according to Fiès & Braund (1998). The modal pore of coarser particles
253　(Rc) was more than three times higher in CHL than in SRP ($p<0.05$, n=12). The packing density of coarser
254　particles, i.e. silt and sand, was similar, with no effect of the origin of HAs, and corresponded to orthorhombic-
255　rhombohedral particle arrangement (Lal & Shukla, 2004).

7

256

*Properties of the colloidal phases*

The colloidal behaviour greatly differed between samples. The CDR values were <0.4 in CHL and >0.8 in SRP (p<0.05, n=12, Table 3), thus less than 40% clay was water dispersible (WDC) in CHL and more than 80% in SRP. The electrophoretic mobility of WDC varied as a function of pH from +0.25 to -0.65 µm cm s$^{-1}$ V$^{-1}$ in CHL; in SRP from +0.27 to -0.52 µm cm s$^{-1}$ V$^{-1}$ (Figure 3). No effect of the origin of HAs was visible in CHL, while in SRP the addition of HA-SRP induced a lower electrophoretic mobility at the lowest pH than HA-CHL (p<0.05, n=6). The point of zero charge (PZC) of both samples was however around pH 2-2.5, and only slightly lower (<2) in the case of SRP with HA-SRP. At the lowest pH, the hydrodynamic diameter of CHL particles was on average slightly smaller than that of SRP (Table 3), and with increasing pH, changes in the electrophoretic mobility were accompanied by a decrease in particle size.

The size of Rf, i.e. the modal radius of voids originated by the arrangement of clay particles, was always lower than 0.02 µm and its variability was small among samples (data not shown). The volume of the modal fine pores (V$_{Hg}$f) was small, and CHL had lower values than SRP (Table 3). The packing density of the clay phase was instead significantly higher in CHL (p<0.05, n=12), and solids may occupy as much as 87-94% of the total volume, corresponding to a very close rhombohedral arrangement of clays.

*HA addition effect*

In order to compare the results obtained in the four treatments (i.e. two soils and two HAs), hence to understand both the effect of HA addition and differing mineralogical composition, the data were matched to those obtained in a previous experiment in which the wet-dry cycle was performed with deionized water only (Falsone et al., 2007).

The mass of the 2-5 mm NF aggregates generally increased after the addition of HA with respect to the water-only wet-dry cycle (Figure 4A). SRP showed the smallest positive variation, but no significant differences among samples were visible. Aggregate stability (both WAS and WAS$_{et}$ indexes) was negatively or poorly affected by HA addition in SRP (Figure 4B, C). This was coupled with a decrease in the volume of coarser pores and an increase in packing density of coarser fraction (Figure 4D, E). Instead CHL HA-added samples were more stable to water abrasion (i.e. WAS$_{et}$ increased), and no variations in V$_{Hg}$C and PDc were found. The results obtained in CHL were thus generally significantly different (p<0.05, n=12) from those in SRP (Figure 4). The differences at macroaggregate scale hence appeared more related to the soil mineralogical composition. A significantly different response between samples (p<0.05, n=12) was also found for the colloidal phase. In fact, with respect to the water-only wet-dry cycle, the dispersibility and size at the lowest pH of the clay fraction of HA-added SRP samples increased (Figure 5A, E) and the PZC decreased (Figure 5D). The V$_{Hg}$f increased in SRP (Figure 5B) and the clay particles had a more open arrangement than in the case of the wet-dry cycle incubation (Figure 5C). In CHL an opposite trend was generally observed, with the exception of PZC values. In fact, upon HA addition, the PZC was reached at lower pH also in CHL although the differences were smaller than in SRP. No significant differences related to the HA origin were observed, with the exception of the

8

293      hydrodynamic diameter (Figure 5).

294

295

296      **DISCUSSION**

297      Differences in sample response upon addition of organic matter, at both macroaggregate and colloidal size

298      scale, were found to be largely dependent on mineralogical composition. The serpentinitic soil (SRP) had a

299      higher macroaggregate formation capacity, and aggregates were more stable than in the chloritic one (CHL),

300      especially against slaking losses. Moreover, the colloidal phase was less dispersible and WDC had a higher

301      electrophoretic mobility in CHL than SRP, although both had a relatively low negative charge with respect to

302      the most common Al-phyllosilicates (Celi et al., 1999). All these findings reflect the aggregation pathways

303      observed in the previous experiment on the effect of wet-dry cycles that can be summarized as dominated by

304      clay-clay interactions in CHL and clay-sand interactions in SRP (Falsone et al., 2007).

305      With respect to the water-only wet-dry cycle, the addition of oxidized organic matter enhanced aggregate

306      formation in both samples but improved aggregate stability towards abrasion only in CHL. In addition, the

307      clay fraction of HA-added CHL samples was less dispersible, although only slight differences in charge

308      properties of the dispersed particles were visible. The $V_{Hg}f$ decreased in CHL and the clay particles had a

309      denser arrangement than in the case of the previous experiment. In HA added SRP an opposite trend was

310      observed, and generally the differences were more pronounced, with a PZC at lower pH and larger

311      hydrodynamic diameter than the water-only wet-dry treated SRP samples. The addition of humic substances

312      on soil (Plaza et al., 2014), oxides (Li et al., 2015) and clay minerals (Majzik & Tombácz, 2007) has a strong

313      effect on surface charge and particle dispersibility, mostly because of the polyelectrolyte nature of HA that

314      increases the net negative charge. The higher flocculation in CHL may be related to a larger abundance of

315      reactive clay surfaces (Vogel et al., 2014), also favoured by the greater presence of Ca on the exchange

316      complex, which can thus form more stable bonds with the organic material (Bronick & Lal, 2005). In CHL,

317      clay particles and HA could thus form a more compact arrangement through clay-Ca-HA, as shown by the PDf

318      increase. The possibility of direct bonding between negatively charged clay surfaces and positive amino groups

319      of proteinaceous remains, abundant in HA-CHL, as well as the interaction of $–COO^-$ groups with mineral edge

320      Me–OH by ligand exchange, cannot be ruled out from electrophoretic mobility data, but cation bridges seem

321      to dominate as no differences between the two HAs were found. Calcium bridges may therefore add to clay-

322      clay interactions in aggregate formation and contribute to the greater stability against abrasion in CHL. The

323      added organic material contribute therefore in this soil to the aggregation process while, being retained into

324      aggregates, had little or no effect on the water dispersible fraction.

325      The larger abundance of Mg, more hydrated than Ca, in the SRP soil might have favoured instead weaker

326      outer-sphere interactions with HA. The presence of HA on clay surfaces has probably hindered the formation

327      of clay coatings on sand grains (Falsone et al. 2007), decreasing aggregate stability and allowing the dispersion

328      of more negatively charged mineral-HA associated particles with respect to the water-only wet-dry conditions.

329      The chemical composition of HA influenced therefore the charge characteristics of WDC: the higher contents

of amino groups in HA-CHL than in HA-SRP induced a higher positive charge at low pH, while the higher carboxyl content made the surfaces more negative at pH higher than the point of zero charge. Phenolic groups may contribute to the negative charge only at pH > 6.0 (Alvarez-Puebla & Garrido, 2005) justifying the less negative electrophoretic mobility obtained with HA-SRP at pH 4.0. As upon HA addition the surface of WDC still carried a positive charge at low pH, stable bonds such as ligand exchange may be ruled out. In addition, since low amounts of HA are sufficient to reverse the mineral charge even at low pH, the amount of HA on clay surfaces was probably very low (Magnacca et al., 2014).

## CONCLUSIONS

Organic matter inputs on the fine earth fraction of a serpentinitic and a chloritic soil promoted the formation of new aggregates in the size range of 2-5 and >5 mm, even if their wet stability was not always positively affected. The soil response however mostly depended on mineralogical composition, with no effect of HA composition on aggregates but only on the surface charge of the dispersible clay particles.

In soils dominated by Mg-silicates, weak chemical interactions between organic matter and mineral particles are the most important mechanism in controlling both aggregation processes and clay dispersibility. Ligand exchange reactions, if any, seem to be of only minor importance, stressing the differences with Al-silicates.

Because of the complex interlink between mineralogy, organic matter characteristics and dominant cations, the addition of organic matter may even favour the dispersion of OM-loaded clay particles, confounding the expected positive effects against land degradation.

## REFERENCES

Abiven S, Menasseri S, Chenu C. 2009. The effects of organic inputs over time on soil aggregate stability – A literature analysis. Soil Biology and Biochemistry 41: 1-12. DOI: 10.1016/j.soilbio.2008.09.015

Adhikari K, Hartemink AE. 2016. Linking soils to ecosystem services – A global review. Geoderma 262: 101-111. DOI: 10.1016/j.geoderma.2015.08.009

Alvarez-Puebla RA, Garrido JJ. 2005. Effect of pH on the aggregation of a gray humic acid in colloidal and solid state. Chemosphere 59: 659-667. DOI: 10.1016/j.chemosphere.2004.10.021

Andruschkewitsch R, Geisseler D, Dultz S, Joergensen RG, LudwigB.2014. Rate of soil-aggregate formation under different organic matter amendments - a short-term incubation experiment. Journal of Plant Nutrition and Soil Science 177: 297-306. DOI: 10.1002/jpln.201200628297

Arjmand Sajjadi S., Mahmoodabadi M. 2015. Aggregate breakdown and surface seal development influenced by rain intensity, slope gradient and soil particle size. Solid Earth 6: 311-321. DOI: 10.5194/se-6-311-2015

367 Berendse F, van Ruijven J, Jongejans E, Keesstra S. 2015. Loss pf plant species diversity reduces soil
368     erosion resistance. Ecosystems 18: 881-888. DOI: 10.1007/s10021-015-9869-6

369 Brevik EC, Cerdà A, Mataix-Solera J, Pereg L, Quinton JN, Six J, Van Oost K. 2015. The interdisciplinary
370     nature of *SOIL*. SOIL 1: 117-129. DOI:10.5194/soil-1-117-2015

371 Bronick CJ, Lal R. 2005. Soil structure and management: a review. Geoderma 124: 3-22. DOI:
372     10.1016/j.geoderma.2004.03.005

373 Bruand A, Prost R. 1987. Effect of water content on the fabric of soil material: an experimental approach.
374     European Journal of Soil Science 38: 461–472. DOI: 10.1111/j.1365-2389.1987.tb02281.x

375 Celi L, Lamacchia S, Ajmone Marsan F, Barberis E. 1999. Interaction of inositol hexaphosphate on clays:
376     Adsorption and charging phenomena. Soil Science 164: 574-585.

377 Cerdà, A. 1996. Soil aggregate stability in three Mediterranean environments. Soil Technology 9: 133-140.
378     DOI: 10.1016/S0933-3630(96)00008-6

379 Cerdà A. 2000. Aggregate stability against water forces under different climates on agriculture land and
380     scrubland in southern Bolivia. Soil and Tillage Research 36: 1- 8. DOI: 10.1016/S0167-
381     1987(00)00155-0

382 Chaplot V, Cooper M. 2015. Soil aggregate stability to predict organic carbon outputs from soils. Geoderma
383     243-244: 205-213. DOI: 10.1016/j.geoderma.2014.12.013

384 Chen Y, Senesi N, Schnitzer M. 1977. Information provided on humic substances by E4/E6 ratios. Soil
385     Science Society of America Journal 41: 353-358. DOI:10.2136/sssaj1977.03615995004100020037x

386 Denef K, Six J, Merckx R, Paustian K. 2002. Short-term effects of biological and physical forces on
387     aggregate formation in soils with different clay mineralogy. Plant and Soil 246: 185-200. DOI:
388     10.1023/A:1020668013524

389 Debasish-Saha,  Kukal SS, Bawa SS. 2014. Soil organic carbon stock and fractions in relation to land use
390     and soil depth in the degraded Shiwaliks hills of lower Himalayas. Land Degradation and
391     Development 25: 407–416.  DOI: 10.1002/ldr.2151

392 De Clercq T, Heiling M, Dercon G, Resch C, Aigner M, Mayer L, Mao Y, Elsen A, Steier P, Leifeld J,
393     Merckx R. 2015. Predicting soil organic matter stability in agricultural fields through carbon and
394     nitrogen stable isotopes. Soil Biology and Biochemistry 88: 29-38. DOI: 0.1016/j.soilbio.2015.05.011

395 de Oliveira SP, de Lacerda N B, Blum SC, Escobar MEO, de Oliveira TS. 2015., Organic Carbon and
396     Nitrogen Stocks in Soils of Northeastern Brazil Converted to Irrigated Agriculture, Land Degradation
397     and Development 26: 9–21. DOI: 10.1002/ldr.2264

398 Ding GC, Geertje JP, Babin D, Heuer H, Heister K, Kögel-Knabner I, Smalla K. 2013. Mineral composition
399     and charcoal determine the bacterial community structure in artificial soils. FEMS Microbiology
400     Ecology 86: 15-25. DOI:10.1111/1574-6941.12070

401 Dong C. 1999. PowderX: Windows-95 based program for powder X-ray diffraction data processing. Journal
402     of Applied Cristallography 32: 838–838. DOI: 10.1107/S0021889899003039

Codice campo modificato

403 Falsone G, Bonifacio E. 2009. Pore-size distribution and particle arrangement in fragipan and nonfragipan
404     horizons. Journal of Plant Nutrition and Soil Science 172:696-703. DOI: 10.1002/jpln.200800066
405 Falsone G, Celi L, Bonifacio E. 2007 Aggregate formation in chloritic and serpentinitic alpine soils. Soil
406     Science 172: 1019-1030. DOI: 10.1097/ss.0b013e31815778a0
407 Fiès JC, Bruand A. 1998: Particle packing and organization of the textural porosity in clay-silt-sand
408     mixtures. European Journal of Soil Science 49: 557–567. DOI: 10.1046/j.1365-2389.1998.4940557.x
409 Gee GW, Bauder JW. 1986. Particle-size analysis. In: Methods of Soil Analysis, Part 1.Physical and
410     Mineralogical Methods. A Klute (ed.). Agron. Monogr. n. 9. ASA and SSSA, Madison, WI, pp. 383–
411     411
412 Gelaw A M, Singh B R, Lal R. 2015. Organic carbon and nitrogen associated with soil aggregates and
413     particle sizes under different land uses in Tigray, northern Ethiopia. Land Degradation and
414     Development 26: 690-700. DOI: 10. 1002/ldr
415 Gümüs I, Şeker C. 2015. Influence of humic acid applications on modulus of rupture, aggregate stability,
416     electrical conductivity, carbon and nitrogen content of a crusting problem soil. Solid Earth 6: 1231-
417     1236. DOI: 10. 5194/se-6-1231-2015
418 Hunter R J. 1986. Foundations of Colloid Science. Vol I. Oxford University Press, New York.
419 Keesstra SD, Geissen V, Mosse K, Piiranen S, Scudiero E, Leistra M, van Schaik L. 2012. Soil as a filter for
420     groundwater quality. Current Opinion in Environmental Sustainability 4: 507-5016. DOI:
421     10.1016/j.cosust.2012.10.007
422 Kögel-Knabner I, Guggenberger G, Kleber M, Kandeler E, Kalbitz K, Scheu S, Eusterhues K, Leinweber P.
423     2008. Organo-mineral associations in temperate soils: Integrating biology, mineralogy, and organic
424     matter chemistry. Journal of Plant Nutrition and Soil Science 171: 61-82.
425     DOI:10.1002/jpln.200700048
426 Lal R, Shukla MK. 2004. Soil Structure. In: Principles of Soil Physics. R Lal and MK Shukla (eds). Marcel
427     Dekker, New York, pp. 93–148
428 Le Bissonnais Y. 1996. Aggregate stability and assessment of soil crustability and erodibility: I. Theory and
429     methodology. European Journal of Soil Science 47: 425–437. DOI: 10.1111/j.1365-
430     2389.1996.tb01843.x
431 Legros JP. 1992. Soils of Alpine mountains. In: Weathering soils and paleosoils. Martini and Chesworth
432     (eds). Developments in Earth Surface Processes, n. 2. Elsevier, Amsterdam, 155-181.
433 Li Y, Yang C, Guo X, Dang Z, Li X, Zhang Q. 2015. Effects of humic acids on the aggregation and sorption
434     of nano-TiO$_2$. Chemosphere 119: 171-176. DOI: 10.1016/j.chemosphere.2014.05.002
435 Majzik A, Tombácz E. 2007. Interaction between humic acid and montmorillonite in the presence of calcium
436     ions I. Interfacial and aqueous phase equilibria: adsorption and complexation. Organic Geochemistry
437     38: 1319-1329. DOI: 10.1016/j.orggeochem.2007.04.003
438 Magnacca G, Allera A, Montoneri E, Celi L, Benito DE, Gagliardi LG, Gonzalez MC, Mártire DO, Carlos L.
439     Novel magnetite nanoparticles coated with waste-sourced biobased substances as sustainable and

12

440 renewable adsorbing materials. ACS Sustainable Chemistry and Engineering 2: 1518-1524. DOI:
441 10.1021/sc500213j

442 Mamedov AI, Bar-Yosef B, Levkovich I, Rosenberg R, Silber A, Fine P, Levy GJ. 2014. Amending soil with
443 sludge, manure, humic acid, orthophosphate and phytic acid: Effects on aggregate stability. Soil
444 Research 52: 317-326. DOI: 10.1071/SR13334

445 Mataix-Solera J, Cerdà A, Arcenegui V, Jordán A, Zavala LM. 2011. Fire effects on soil aggregation: A
446 review. Earth-Science Reviews 109: 44-60. DOI: 10.1016/j.earscirev.2011.08.002

447 Mikutta R, Mikutta C, Kalbitz K, Scheel T, Kaiser K, Jahn R. 2007. Biodegradation of forest floor organic
448 matter bound to minerals via different binding mechanisms. Geochimica et Cosmichimica Acta 71:
449 2569-2590. DOI: 10.1016/j.gca.2007.03.002

450 Mizuta K, Taguchi S, Sato S. 2015. Soil aggregate formation and stability induced by starch and cellulose.
451 Soil Biology and Biochemistry 87: 90-96. DOI: 10.1016/j.soilbio.2015.04.011

452 Muñoz-Rojas M, Jordán A, Zavala LM, De la Rosa D, Abd-Elmabod SK, Anaya-Romero M. 2015. Impact
453 of Land Use and Land Cover Changes on Organic Carbon Stocks in Mediterranean Soils (1956–2007).
454 Land Degradation and Development 25: 168–179. DOI: 10.1002/ldr.2194

455 O'Rourke SM, Angers DA, Holden NM, McBratney AB. 2015. Soil organic carbon across scales. Global
456 Change Biology. DOI: 10.1111/gcb.12959,

457 Piccolo A, Mbagwu JSC. 1999. Role of hydrophobic components of soil organic matter on the stability of
458 soil aggregates. Soil Science Society of America Journal 63: 1801–1810.
459 DOI:10.2136/sssaj1999.6361801x

460 Plaza I, Ontiveros-Ortega A, Calero J, Aranda V. 2014. Implication of zeta potential and surface free energy
461 in the description of agricultural soil quality: effect of different cations and humic acids on degraded
462 soils. Soil and Tillage Research 146: 148-158. DOI: 10.1016/j.still.2014.10.013

463 Regelink IC, Stoof CR, Rousseva S, Weng L, Lair GJ, Kram P, Nikolaidis NP, Kercheva M, Banwart S,
464 Comans RNJ 2015. Linkages between aggregate formation, porosity and soil chemical properties.
465 Geoderma 247-248: 24-37. DOI: 10.1016/j.geoderma.2015.01.022

466 Schnitzer ME, Gupta VC. 1965. Determination of acidity in soil organic matter. Soil Science Society of
467 America Proceedings 29: 274-277

468 Seeger M, Ries JB. 2008. Soil degradation and soil surface process intensities on abandoned fields in
469 Mediterranean mountain environments. Land Degradation and Development 19: 488–501, DOI:
470 10.1002/ldr.854

471 Six J, Paustian K. 2014. Aggregate-associated soil organic matter as an ecosystem property and a
472 measurement tool. Soil Biology and Biochemistry 68: A4-A9. DOI: 10.1016/j.soilbio.2013.06.014

473 Six J, Bossuyt H, Degryze S, Denef K. 2004. A history of research on the link between (micro)aggregates,
474 soil biota, and soil organic matter dynamics. Soil and Tillage Research 79: 7-31. DOI:
475 10.1016/j.still.2004.03.008

476  Stanchi S, Falsone G, Bonifacio E. 2015. Soil aggregation, erodibility, and erosion rates in mountain soils
477  (NW Alps, Italy). Solid Earth 6: 403–414. DOI: 10.5194/se-6-403-2015

478  Soil Survey Staff. 2014. Keys to Soil Taxonomy, 12th ed. USDA-Natural Resources Conservation Service,
479  Washington, DC.

480  Swift RS. 1996. Organic matter characterization. In: Methods of Soil Analysis: Chemical Methods, 3rd Ed.
481  D. L Sparks (ed.). ASA and SSSA, Madison, WI, pp. 1011–1070

482  Vogel C, Babin D, Pronk GJ, Heister K, SmallaK, Kögel-Knabner I. 2014. Establishment of macro-
483  aggregates and organic matter turnover by microbial communities in long-term incubated artificial
484  soils. SoilBiology and Biochemistry 79: 57-67. DOI:10.1016/j.soilbio.2014.07.012

485  Vogel C, Mueller CW, Höschen C, Buegger F, Heister K., Schulz S, Schloter M, Kögel-Knabner I. 2014.
486  Submicron structures provide preferential spots for carbon and nitrogen sequestration in soils. Nature
487  Communications 5: 2947. DOI:10.1038/ncomms3947

488  Zhang K, Zheng H, Chen FL, Ouyang ZY, Wang Y, Wu YF, Lan J, Fu M, Xiang XW. 2015. Changes in soil
489  quality after converting Pinus to Eucalyptus plantations in southern China. Solid Earth 6: 115-123.
490  doi:10.5194/se-6-115-2015

491  Zornoza R, Acosta JA, Bastida F, Domínguez SG, Toledo DM, Faz A. 2015. Identification of sensitive
492  indicators to assess the interrelationship between soil quality, management practices and human
493  health. SOIL 1: 173-185. DOI:10.5194/soil-1-173-2015

494

Table 1. Mean (± standard deviation) of elemental content, total acidity, carboxyl groups, and $E_4/E_6$ ratio of purified, ash and moisture-free HAs extracted from the CHL and SRP organic horizons (HA-CHL and HA-SRP, respectively). The letters show the significant differences at $p$ level <0.05 (Duncan's test) between HA (n=6)

| | HA-CHL | HA-SRP |
|---|---|---|
| ash (%) | 1.6±0.3 | 1.2±0.1 |
| C (%) | 50.51±0.31[b] | 54.59±0.61[a] |
| N (%) | 5.51±0.27[a] | 3.59±0.26[b] |
| H (%) | 6.13±0.04 | 6.16±0.09 |
| S (%) | 0.64±0.01[a] | 0.30±0.03[b] |
| O (%) | 37.21±0.33 | 35.35±0.80 |
| C/N | 10.69±0.54[b] | 17.72±1.07[a] |
| H/C | 1.45±0.01[a] | 1.35±0.04[b] |
| O/C | 0.55±0.01[a] | 0.49±0.02[b] |
| total acidity (cmol kg$^{-1}$) | 566±8[b] | 608±11[a] |
| -COOH (cmol kg$^{-1}$) | 254±6[a] | 232±3[b] |
| Phenolic OH (cmol kg$^{-1}$) | 312±1[b] | 376±8[a] |
| $E_4/E_6$ | 6.20±0.08[b] | 6.57±0.08[a] |

-COOH: carboxyl groups; Phenolic OH: phenolic OH-groups; $E_4/E_6$: ratio of absorbance at 465 and 665 nm

502 Table 2. Mean (± standard deviation) of percentage of newly-formed aggregate classes and aggregate Mean

503 Weight Diameter (MWD). The letters show the significant differences at *p* level <0.05 (Duncan's test)

504 between treatments within each site (n=6; lowercase letters) and between sites (n=12; uppercase letters)

505

| soil sample | treatment | 2-5 mm (%) | >5 mm (%) | MWD (mm) |
|---|---|---|---|---|
| CHL | HA-CHL | 19.6±1.6 | 9.1±0.7 | 2.08±0.01 |
| | HA-SRP | 17.5±3.6 | 10.3±2.5 | 2.10±0.23 |
| | *mean±st. dev* | 18.8±2.9 [B] | 9.8±1.9[B] | 2.10±0.16[B] |
| SRP | HA-CHL | 33.2±3.4[a] | 14.4±1.6 | 2.77±0.19 |
| | HA-SRP | 27.4±2.5[b] | 15.9±4.6 | 2.72±0.28 |
| | *mean±st. dev* | 29.7±4.0[A] | 15.3±3.4[A] | 2.74±0.22[A] |

506

507 Table 3. Mean (± standard deviation) of stability indexes of 2-5 mm newly-formed aggregates (WAS and

508 WAS$_{et}$) and of the colloidal phase (CDR), porosity data of coarser particles (i.e. sand and silt), and

509 characteristics of the colloidal phases obtained from newly-formed aggregates. The letters show the

510 significant differences at $p$ level <0.05 (Duncan's test) between treatments within each site (n=6; lowercase

511 letters) and between sites (n=12; uppercase letters)

| soil sample | CHL | | | SRP | | |
|---|---|---|---|---|---|---|
| treatment | HA-CHL | HA-SRP | *mean±dev.st* | HA-CHL | HA-SRP | *mean±dev.st* |
| WAS (%) | 61.0±1.4[b] | 64.9±1.1[a] | 63.0±2.5[B] | 71.6±0.7 | 72.0±1.3 | 71.8±0.9[A] |
| WAS$_{et}$ (%) | 73.8±1.8[a] | 71.8±1.8[b] | 72.8±1.9 | 77.0±1.7[a] | 72.2±2.5[b] | 74.6±3.3 |
| V$_{Hg}$Tot (mm$^3$ g$^{-1}$) | 180±11 | 177±9 | 178±10 | 177±25 | 188±23 | 183±43 |
| V$_{Hg}$c (mm$^3$ g$^{-1}$) | 178±9 | 176±9 | 177±10 | 173±22 | 175±18 | 174±43 |
| Rc (µm) | 1.494±0.272 | 1.809±0.279 | 1.651±0.349[A] | 0.450±0.129 | 0.470±0.012 | 0.460±0.076[B] |
| PDc | 0.67±0.01 | 0.67±0.01 | 0.67±0.01 | 0.68±0.03 | 0.68±0.02 | 0.68±0.05 |
| CDR | 0.38±0.04 | 0.30±0.03 | 0.34±0.06[B] | 0.86±0.05 | 0.94±0.04 | 0.90±0.07[A] |
| hydrodynamic diameter at the lowest pH (µm) | 1.05±0.14[a] | 0.83±0.04[b] | 0.94±0.15 | 0.92±0.10 | 1.08±0.17 | 1.00±0.17 |
| hydrodynamic diameter at the highest pH (µm) | 0.72±0.10 | 0.78±0.07 | 0.75±0.08 | 0.71±0.03 | 0.71±0.02 | 0.71±0.02 |
| V$_{Hg}$f (mm$^3$ g$^{-1}$) | 2±1 | 1±<1 | 1±1 | 5±4 | 14±5 | 9±6 |
| PDf | 0.87±0.08 | 0.94±0.04 | 0.91±0.06[A] | 0.73±0.17 | 0.52±0.09 | 0.62±0.16[B] |

512 WAS: wet aggregate stability; WAS$_{et}$: wet aggregate stability after ethanol saturation; V$_{Hg}$Tot: total volume of intruded

513 Hg (i.e. total pore volume); V$_{Hg}$c: volume of pores within the coarser particles; Rc: modal radius of packing of coarser

514 particles; PDc: packing density of the coarser particles; CDR: clay dispersion ratio; V$_{Hg}$f: volume of pores within the

515 finer particles; PDf: packing density of the finer particles
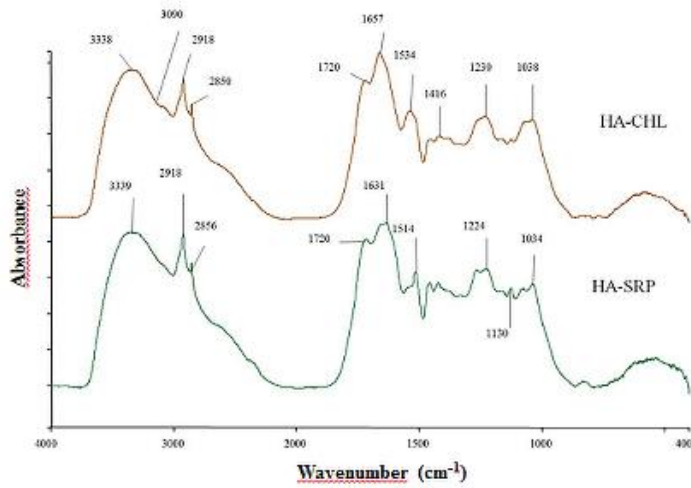
516

**Captions to Figures**

519    Figure 1 – Mineral composition of bulk (<2 mm) and clay fractions of the CHL and SRP soil samples
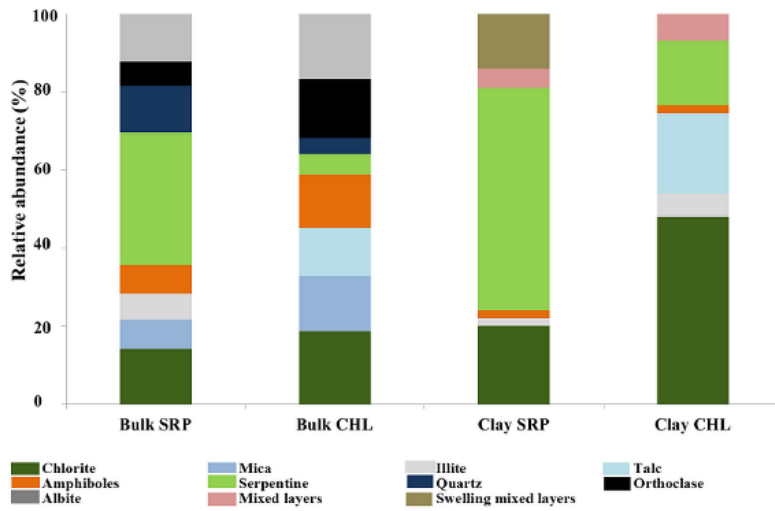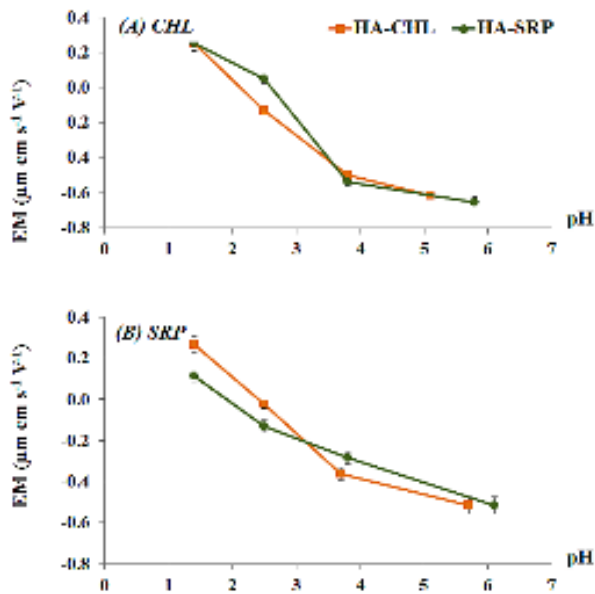


520
521    Figure 2 - FT-IR spectra of humic acids from the topsoil of CHL and SRP



522
523

524 Figure 3 - Electrophoretic mobility (EM) values of WDC fraction of 2-5 NF aggregates obtained after HA

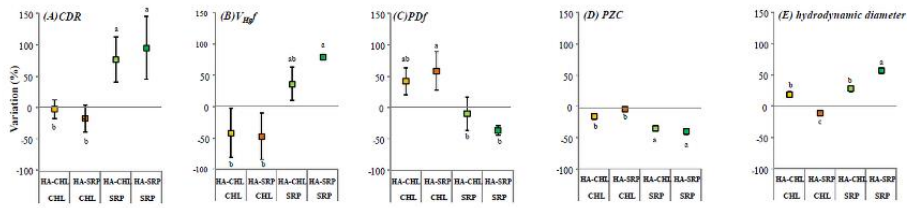525 addition in CHL (A) and SRP (B). Bars represent standard deviation

526



527

528

529 Figure 4 – Variations in the characteristics of 2-5 NF aggregates after HA addition with respect to water-only

530 wet-dry experiment. Percentage changes in mass of aggregates (A), WAS (B), $WAS_{et}$ (C) and porosity data of

531 coarser particles of NF-macroaggregates (D, E). Bars represent standard deviation (SD). For graphical reasons

532 SDs <1% were not reported. The letters show the significant differences at p level <0.05 (Duncan's test) among

533 the four treatments



534

535
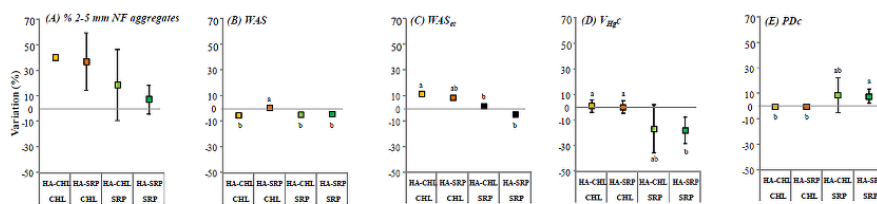
Figure 5 – Variations in the characteristics of water dispersible clay from NF aggregates after HA addition with respect to water-only wet-dry experiment. Percentage changes in CDR (A), porosity data of finer particles (B, C), PZC (D) and equivalent hydrodynamic diameter (E). Bars represent standard deviation (SD). For graphical reasons SDs <5% were not reported. The letters show the significant differences at p level <0.05 (Duncan's test) among the four treatments